Electronic Supplementary Material (ESI) for Dalton Transactions.

A fluorescence 'turn-on' chemodosimeter for specific detection of Pd^{2+} by rhodamine appended Schiff base and its application in live cell imaging

Anup Kumar Bhanja, Snehasis Mishra, Krishna Das Saha and Chittaranjan Sinha*

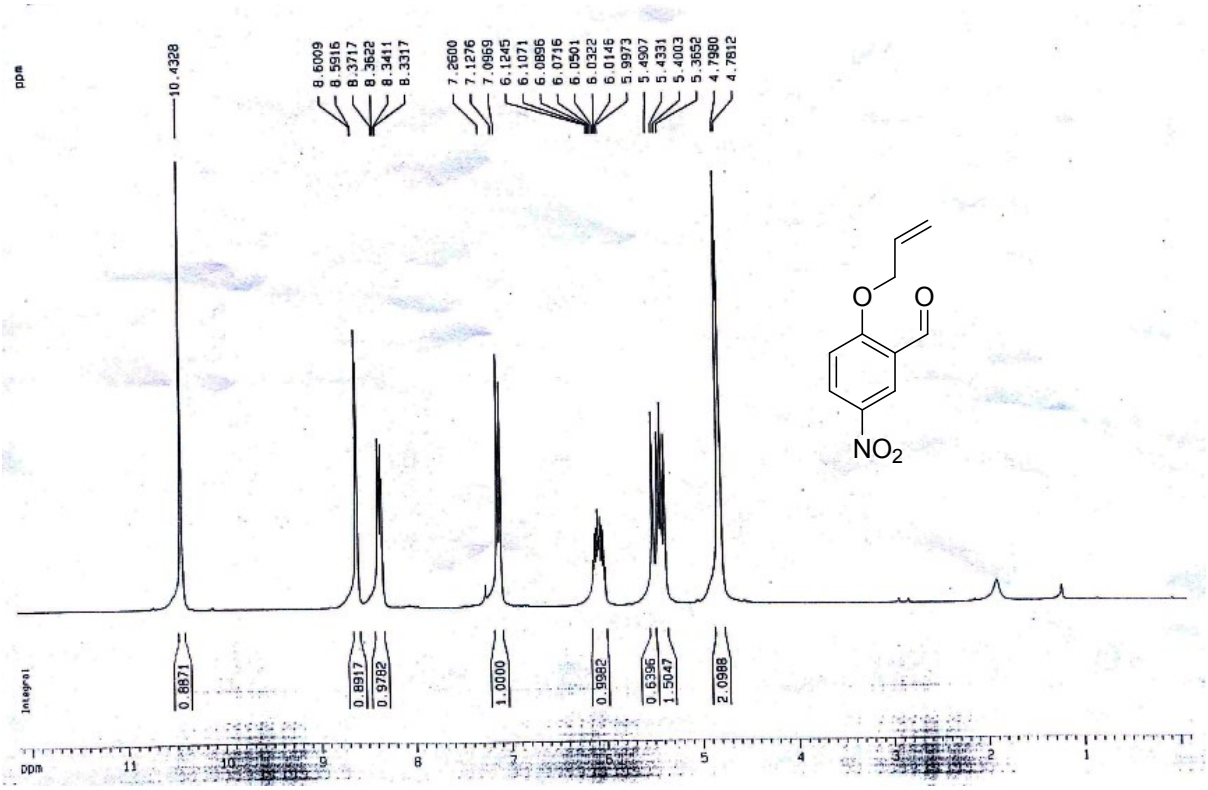

Fig. S1. 1H-NMR of 2-allyloxy-5-nitrobenzaldehyde (**A**).

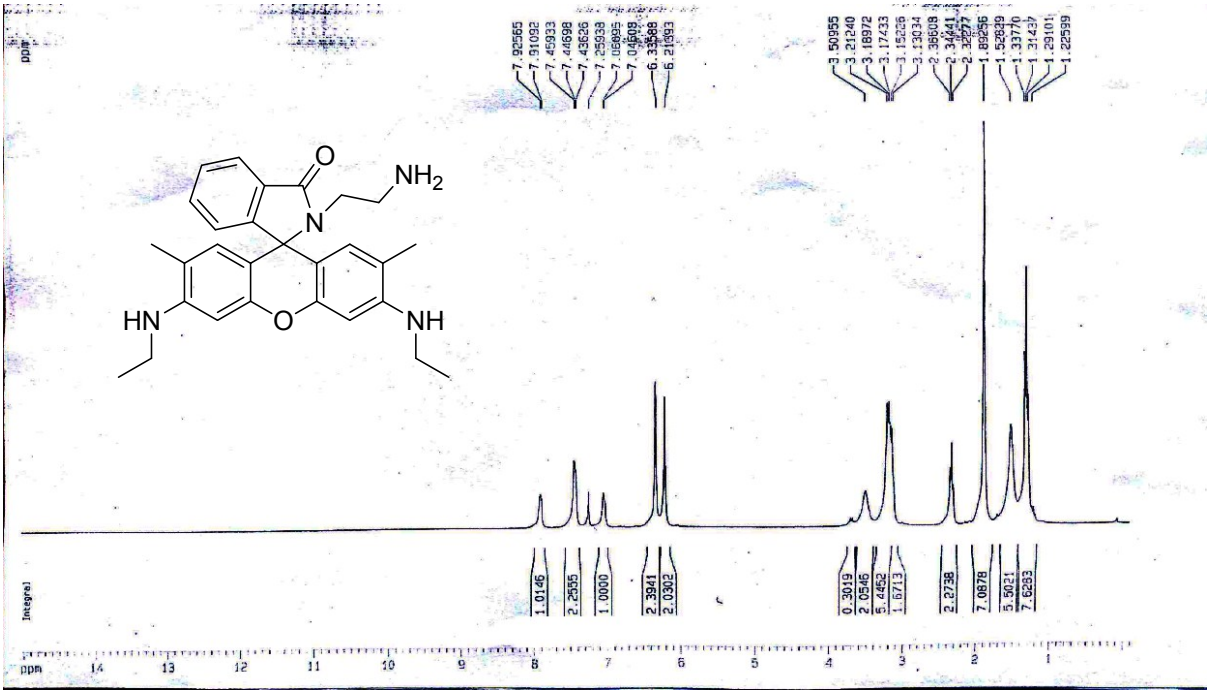

Fig. S2. 1H-NMR of N-(Rhodamine-6G)lactam-ethylenediamine (**B**).

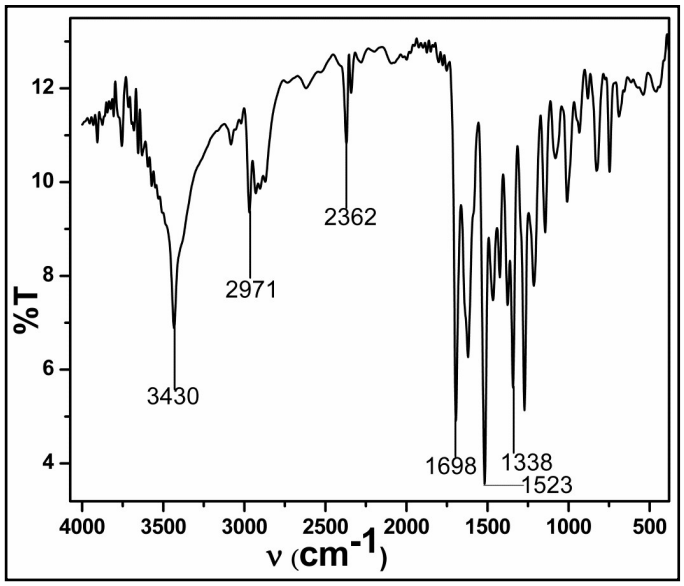

Fig. S3. FT-IR spectrum of RD in KBr disc

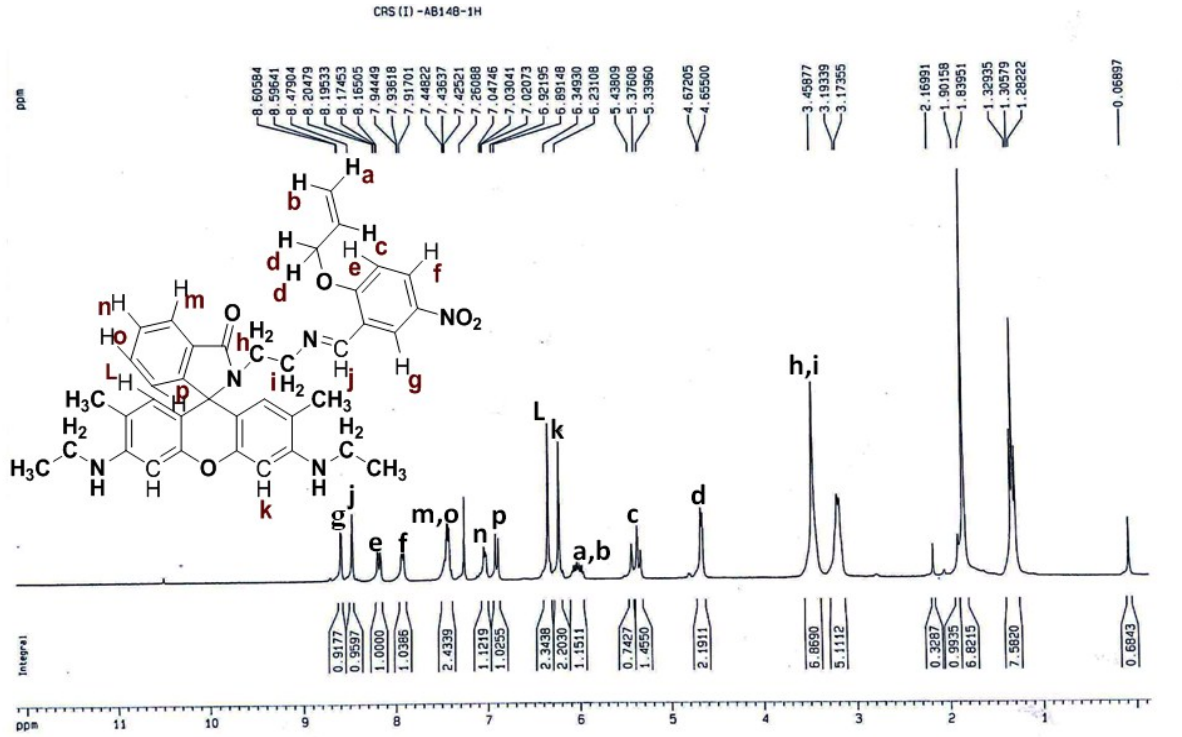

Fig. S4. [1]HNMR spectrum of RD in $CDCl_3$

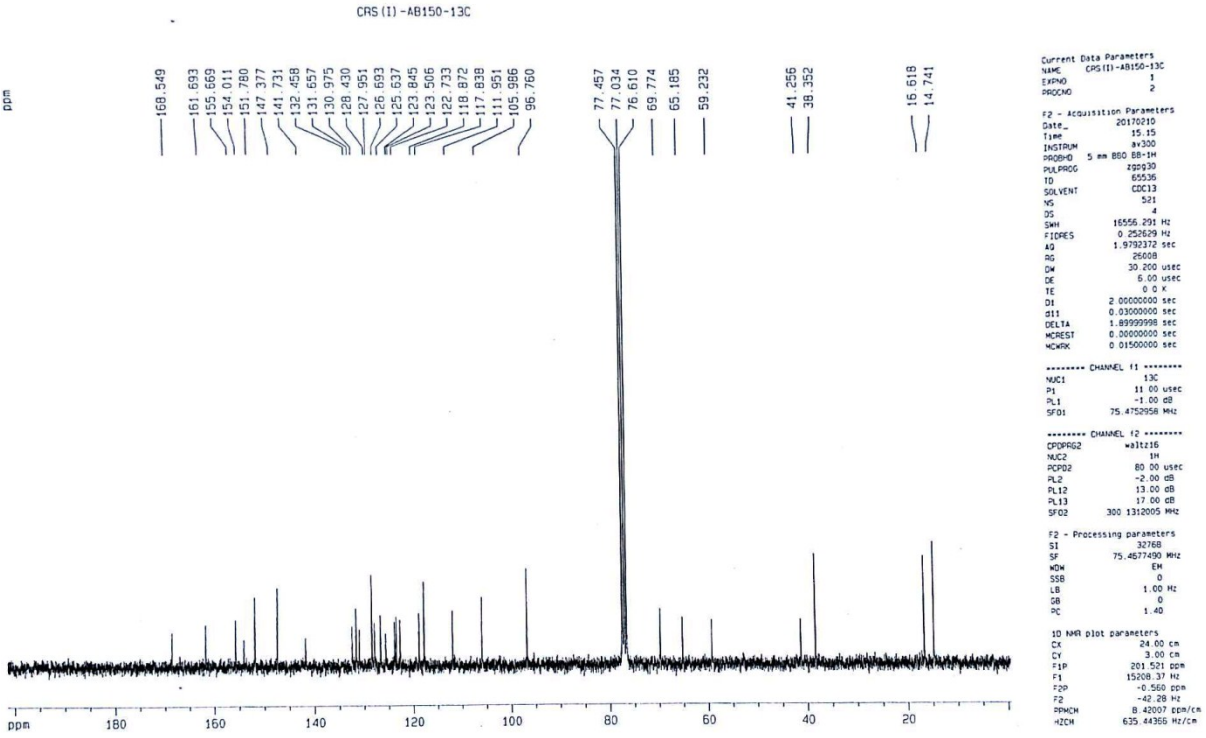

Fig. S5. [13]CNMR spectrum of RD in $CDCl_3$

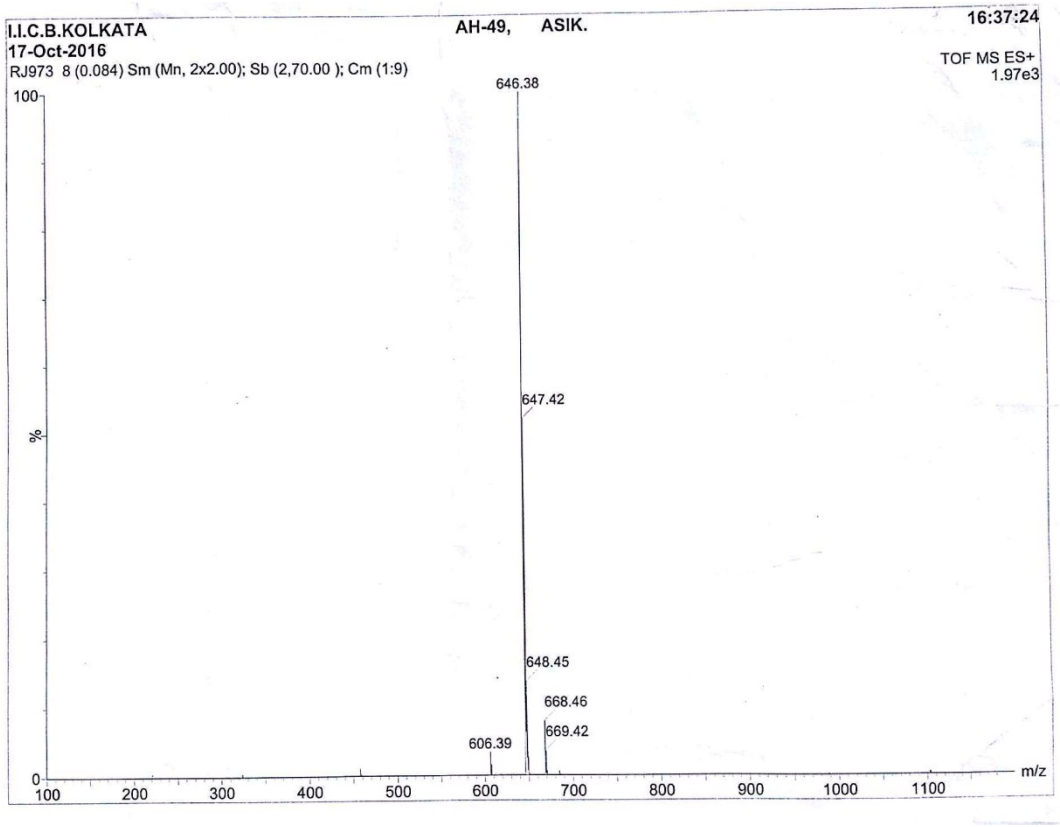

Fig. S6. Mass spectrum of RD

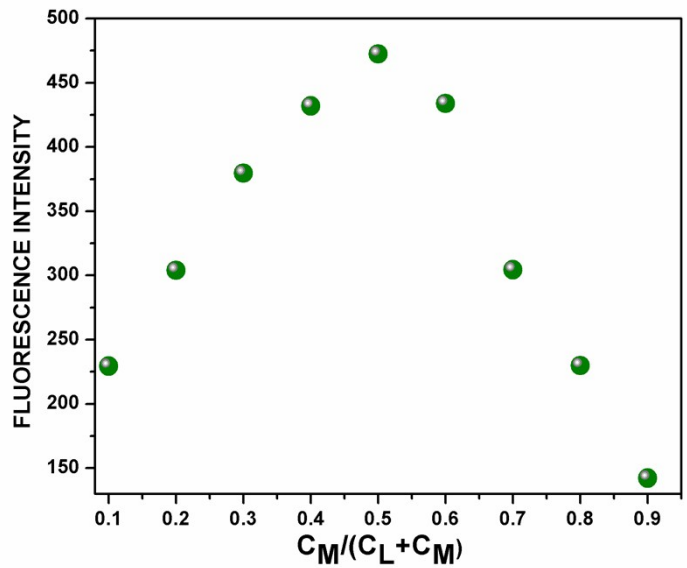

Fig S7. The Job's plot shows 1 : 1 stoichiometry between [Pd^{2+}] and [RD]

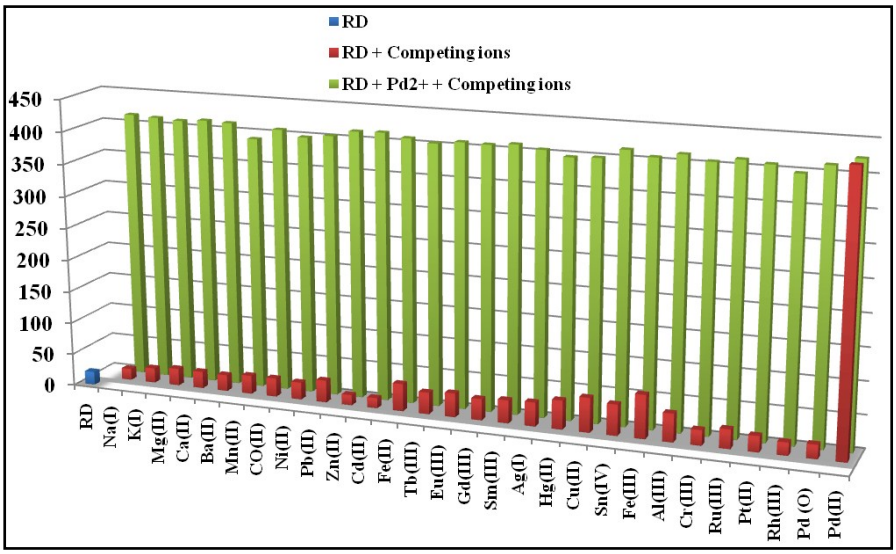

Fig. S8. Fluorescence intensity changes profiles of 100 μM RD in CH_3CN–water (HEPES buffer, pH =7.4; v/v, 1/4) in presence of selected metal ions at excitation wavelength 485 nm.

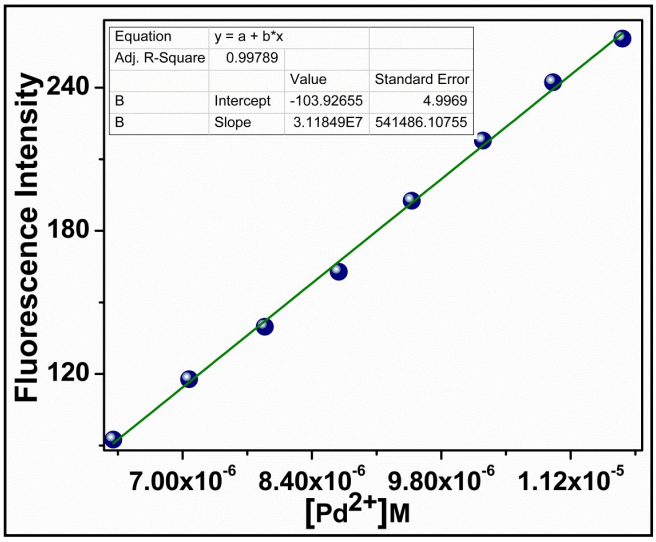

Fig. S9. The linear dynamic response of H_2L for Zn^{2+} and the determination of the detection limit (LOD) for Zn^{2+}

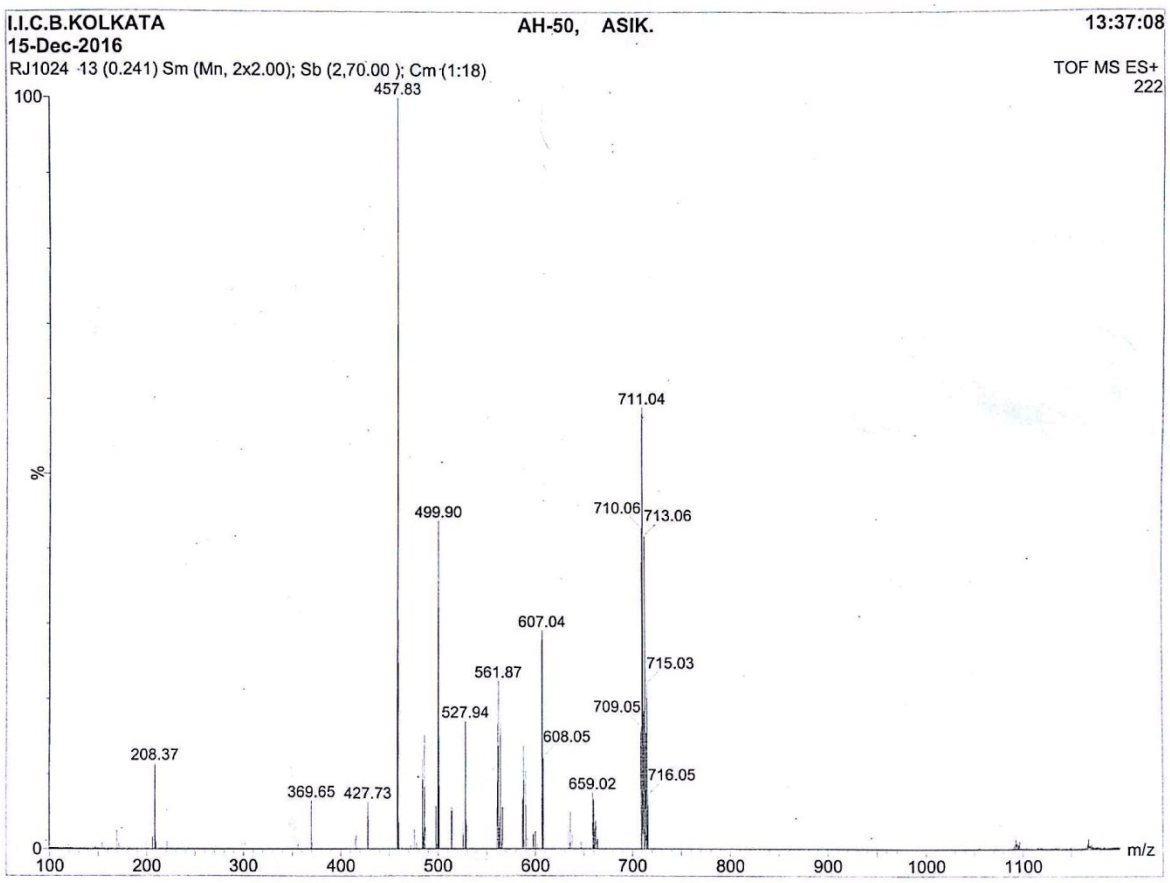

Fig. S10. Mass spectrum of Complex.

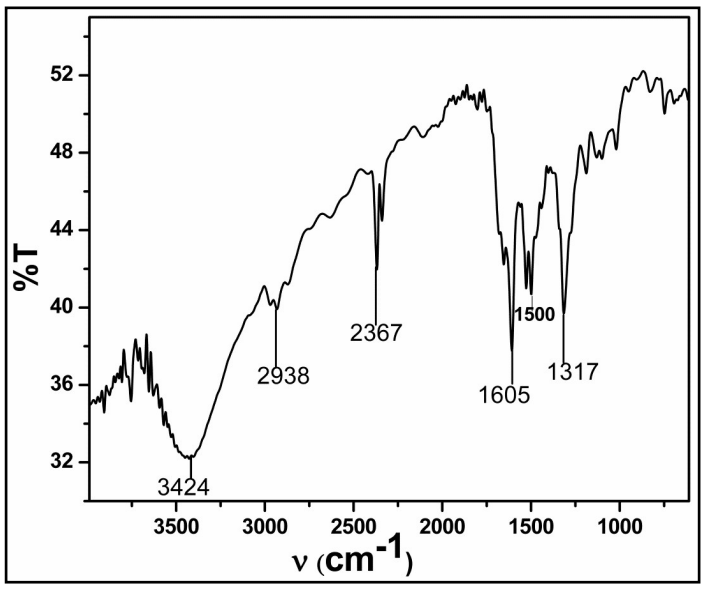

Fig. S11. FT-IR spectrum of Complex in KBr disc

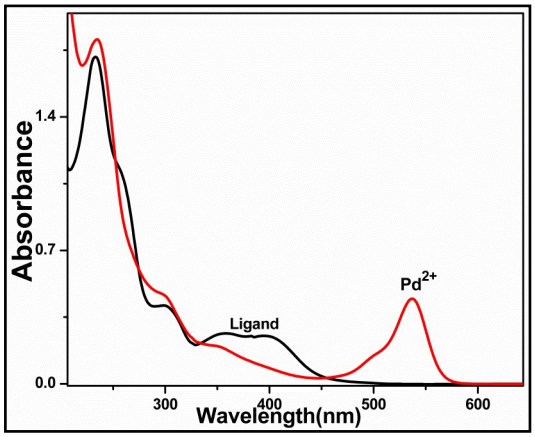

Fig. 12a. UV-Vis absorption spectra of RD' and RD' in presence of Pd^{2+}.

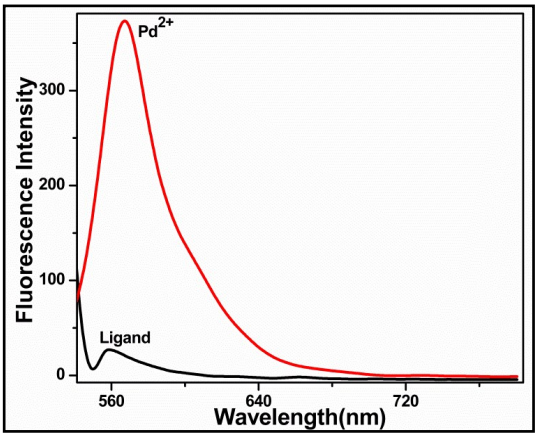

Fig. 12b. Fluorescence spectra of RD' and RD' in presence of Pd^{2+}.

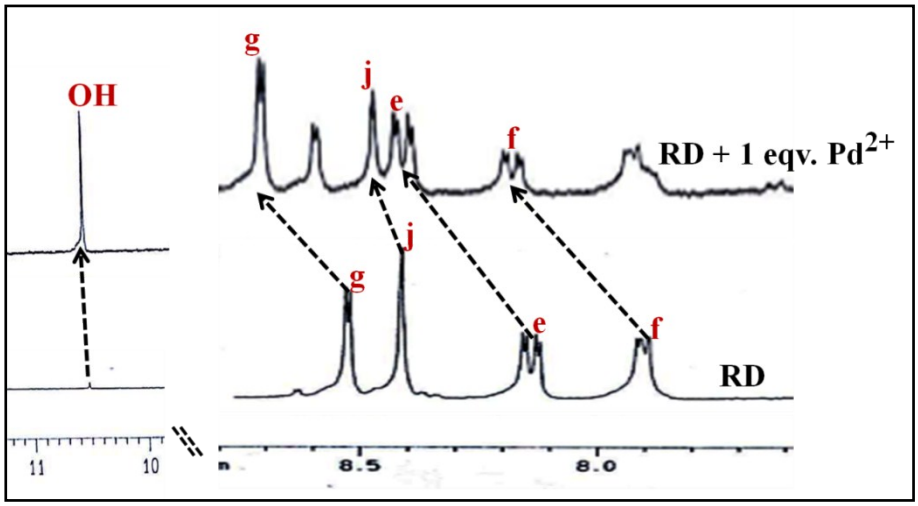

Fig. S13. Partial ^{1}H-NMR spectra (300 MHz, $CDCl_3$) of RD and RD With 1 equiv. of Pd^{2+}

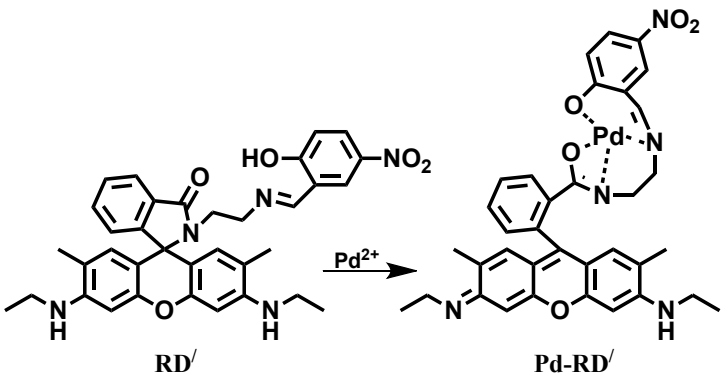

RD/ Pd-RD/

Scheme S1. Structure of RD/ and [Pd-RD/]

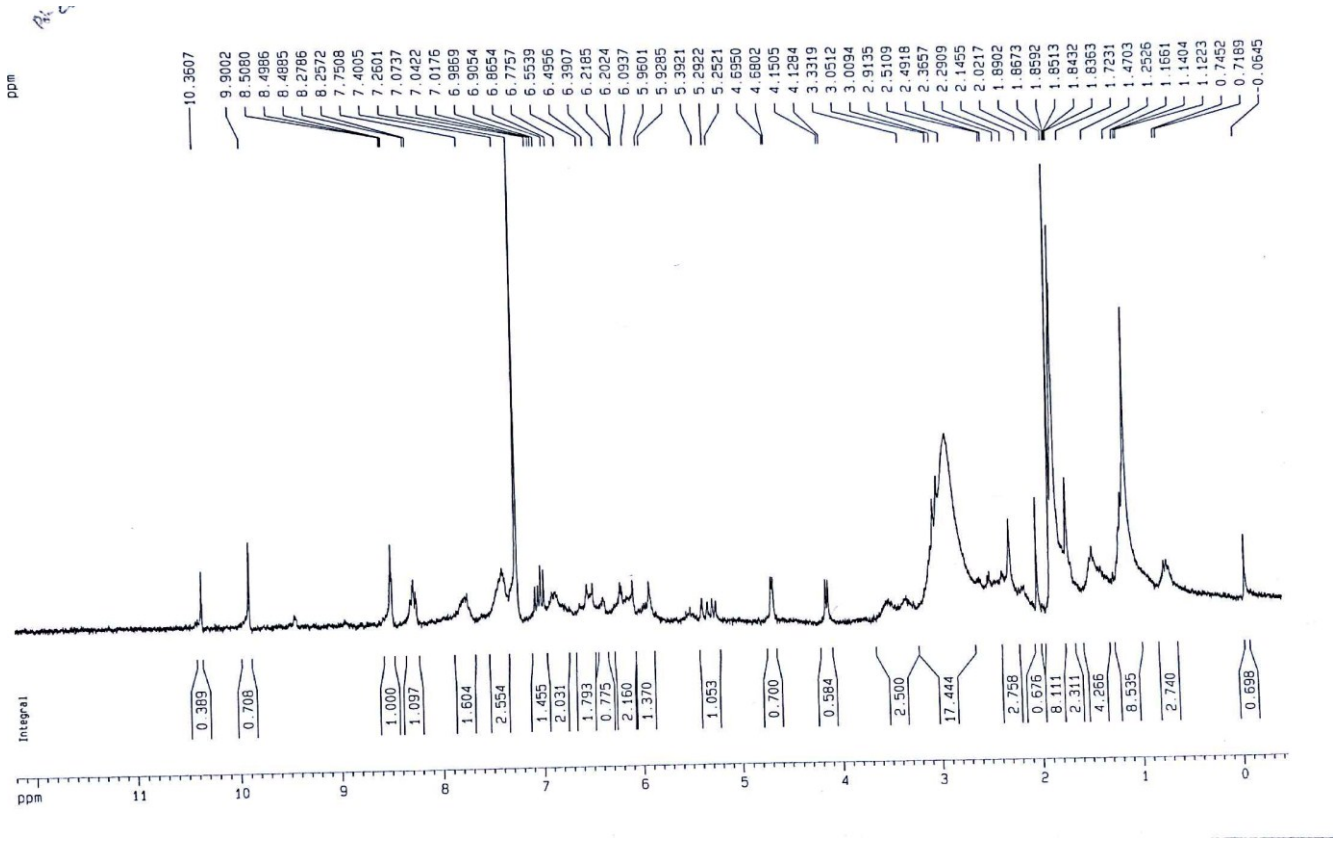

Fig. S14a. ^{1}H NMR spectrum of RD-Pd^{2+} Complex in $CDCl_3$

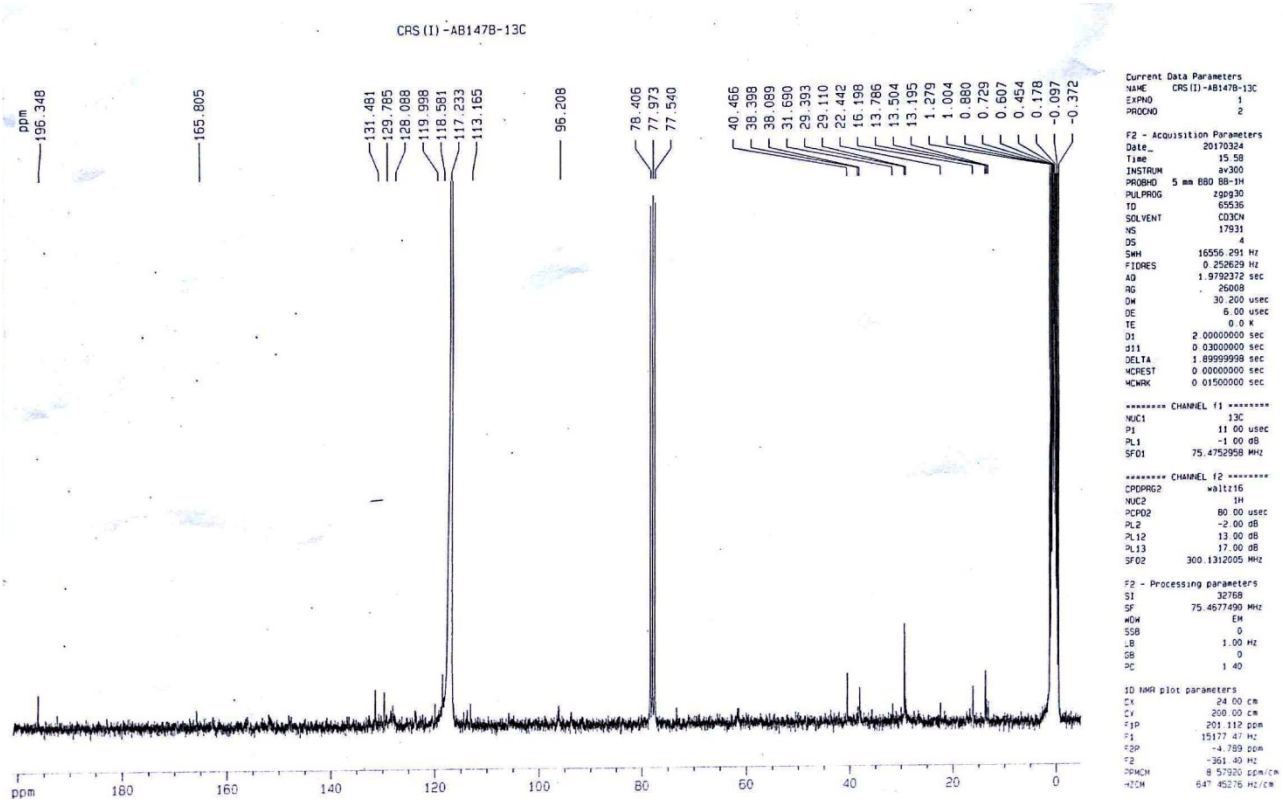

Fig. S14b. ^{13}C NMR spectrum of RD-Pd^{2+} Complex in CD_3CN-$CDCl_3$.

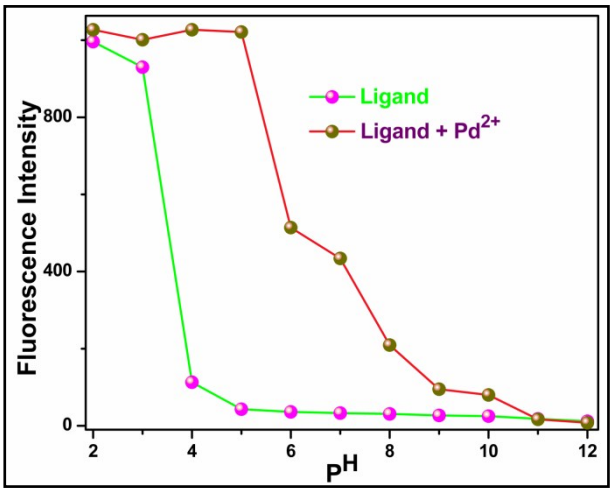

Fig. S15. Effect of pH on the fluorescence activity of RD and RD with Pd^{2+} in (CH_3CN/H_20, ¼, v/v, HEPES buffer).

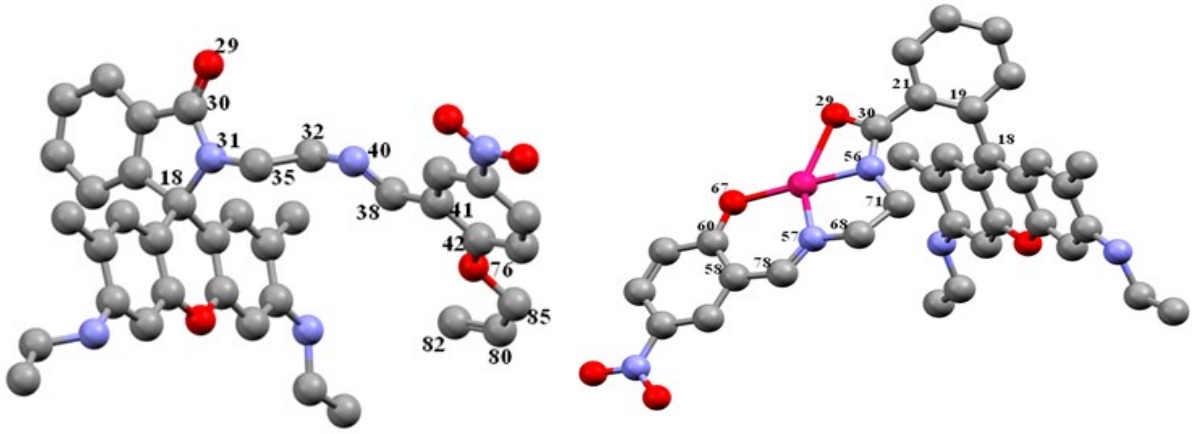

Fig. S16. Optimized structures of RD and RD-Pd^{2+} complex of Rd.

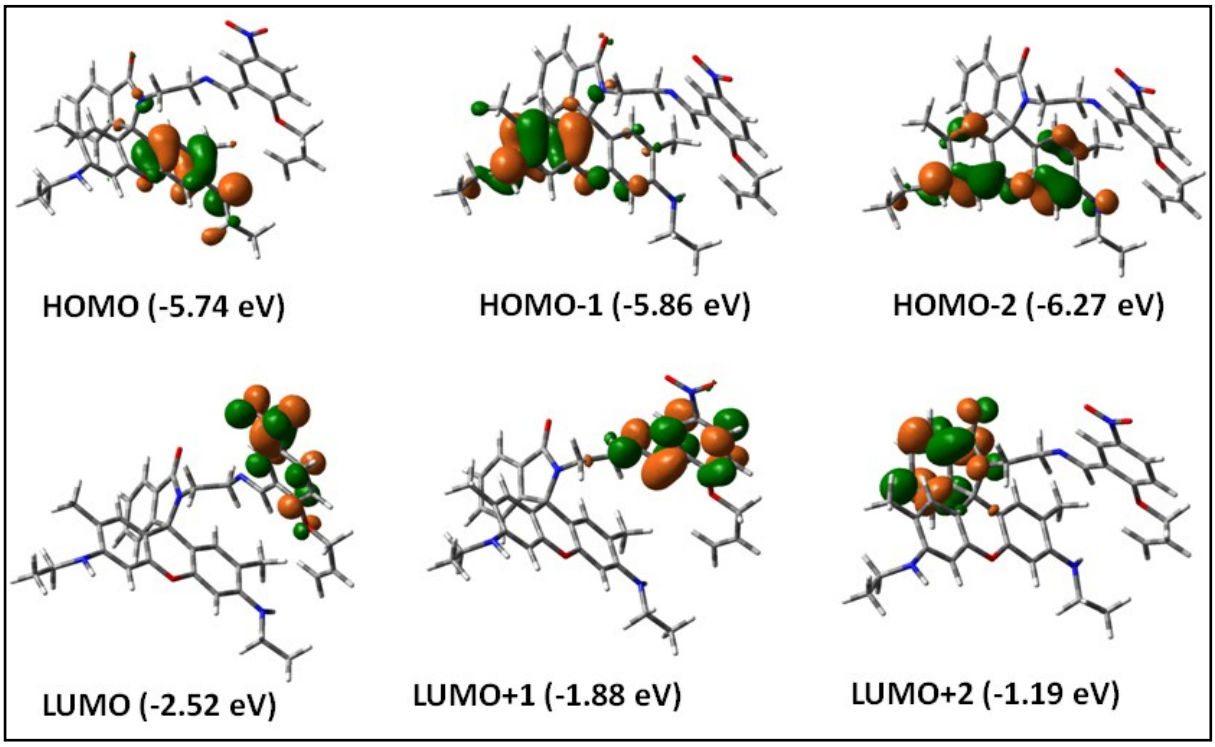

Fig S17: Frontier molecular orbitals of RD

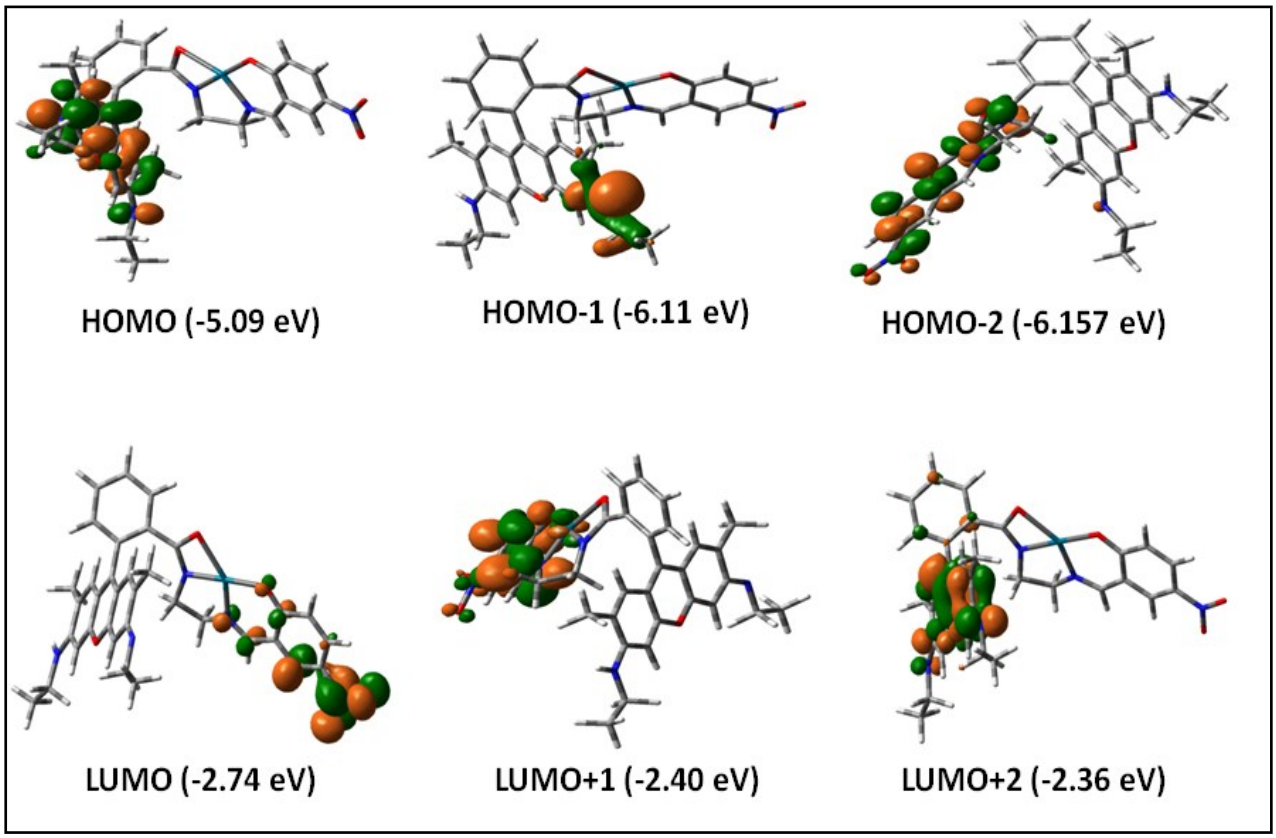

Fig S18: Frontier molecular orbitals of Palladium Complex

Bond Distance (Å)		Bond angle (°)	
C(18)-N(31) C(30)-N(31)	1.493 1.375	C(30)-N(31)-C(35)	121.92
C(30)-O(29) N(31)-C(35)	1.221 1.406	C(18)-N(31)-C(35)	123.57
C(38)-N(40) N(40)-C(32)	1.269 1.450	C(41)-C(38)-N(40)	121.90
O(76)-C(85) C(42)-O(76)	1.425 1.355	C(42)-O(76)-C(85)	119.66

Table S1: Bond parameters of RD

Table S2: Bond parameters of Palladium complex

Bond Distance (Å)		Bond angle (°)	
Pd-O(29) Pd-O(67)	2.316 2.027	O(29)-Pd-O(67) Pd-O(29)-C(30)	119.47 85.68
Pd-N(56) Pd-N(57)	1.952 1.965	N(56)-Pd-N(57) Pd-N(56)-C(30)	84.92 101.79

C(30)-O(29) N(56)-C(30)	1.326 1.335	O(29)-C(30)- N(56) O(67)-Pd- N(57)	111.16 94.45
N(56)-C(71) C(68)-C(71)	1.462 1.551	Pd-N(56)-C(71)	115.33
N(57)-C(68) C(78)-N(57)	1.503 1.303	Pd-N(57)-C(78)	125.58
C(60)-O(67)	1.320	Pd-O(67)-C(60)	123.94

Table S3. Composition and energy of MOs Palladium Complex.

Orbital	Energy(eV)	Composition	
		Metal	Ligand
LUMO+10	0.22	32	68
LUMO+9	-0.18	30	70
LUMO+8	-0.31	54	46
LUMO+7	-0.38	7	93
LUMO+6	-0.54	2	98
LUMO+5	-0.96	0	100
LUMO+4	-1.5	7	93
LUMO+3	-2.18	52	48
LUMO+2	-2.36	1	99
LUMO+1	-2.4	4	96
LUMO	-2.74	1	99
HOMO	-5.09	0	100
HOMO-1	-6.11	0	100
HOMO-2	-6.15	21	79
HOMO-3	-6.36	0	100
HOMO-4	-6.61	1	99
HOMO-5	-6.69	20	80
HOMO-6	-6.9	60	40
HOMO-7	-7.09	50	50
HOMO-8	-7.34	31	69
HOMO-9	-7.37	1	99

HOMO-10	-7.53	0	100